Proceedings of the ASME 2023
International Mechanical Engineering Congress and Exposition
IMECE2023
October 29-November 2, 2023, New Orleans, Louisiana

IMECE2023-112944

NONRECIPROCAL TRANSMISSION OF LAMB WAVES VIA SURFACE-BONDED ELASTIC METAMATERIAL DIODE

Hexuan Xu
University of Michigan-Shanghai Jiao Tong University Joint Institute, Shanghai Jiao Tong University, Shanghai, China

Yanfeng Shen
University of Michigan-Shanghai Jiao Tong University Joint Institute, Shanghai Jiao Tong University, Shanghai, China

ABSTRACT

This paper presents two types of elastic meta-structural functional units with symmetric and antisymmetric layouts, synthetically collaborating for realizing one-way, nonreciprocal transmission of Lamb waves. The elastic meta-structural functional unit cells are comprised of Locally Resonant (LR) cylinders arranged in a periodic pattern bonded on an aluminum plate. The mechanism behind the metamaterial guided wave diode resides in the wave mode manipulation, including mode conversion and selective mode transmission. This study explores with a systematic parametric study on the antisymmetric elastic meta-structural unit cell with various shapes. The optimal configuration is determined from the parametric study to identify the most effective mode conversion performance. Highly effective mode conversion from S_0 mode into A_0 mode can be achieved by the antisymmetric units. The height of the unit cell stub and the amount of unit cells are respectively explored with a finite element model (FEM) using harmonic analysis. The performance of the proposed ultrasound mode convertor is further substantiated via the harmonic analysis of a metamaterial chain model, via showcasing the frequency spectrum of the transmitted wave modes. Subsequently, filtering of symmetric Lamb modes can be achieved by symmetric resonant elastic metamaterial. Modal analysis with Bloch-Floquet boundary condition is performed to obtain the dispersion features of the metamaterial system. By investigating the band structure and the resonant motions, a complete antisymmetric Lamb modes transmission band within the symmetric Lamb modes bandgap can be established in a wide frequency range. Afterwards, an elastic wave diode is constructed by combining the proposed unit cells for the nonreciprocal transmission manipulation of symmetric Lamb waves. The proposed nonreciprocal transmission capability may possess great potential for the purpose of one-way wave control and manipulation.

Keywords: metasurface; wave diode; mode conversion; bandgap; nonreciprocal wave manipulation

1. INTRODUCTION

Lamb waves are a category of guided waves widely used in ultrasonic non-destructive evaluation and structural health monitoring[1, 2]. Ultrasonic Lamb waves possess the advantages of large inspection area and high detection efficiency[3]. Lamb waves can be classified into two types: symmetric Lamb waves and antisymmetric Lamb waves[4]. Each type corresponds to multiple modes with distinctive polarization of particle motion characteristics. The aspects of transmission, reception, and signal processing are extremely complex, which greatly limits its wide application in industry[5, 6]. Unidirectional transmission is of great interest to broad communities, since it allows energy transmission only in one direction with diverse applications[7-9]. The sensitivity of elastic wave monitoring is subject to the frequency and mode of the interrogative wave field. As such, one-way propagation control of waves of specific frequencies and modes is preferable, as it enhances interference resistance and monitoring accuracy in structural health monitoring background settings[10]. Therefore, it is of great significance to investigate the one-way transmission control of specific Lamb modes.

As a new variety of artificial material, elastic metamaterials have excellent mechanical properties that are not found in natural materials, and have shown great potential in the transmission manipulation of elastic waves[11-14]. The propagation of elastic waves is manipulated by periodic structures while being confined within a limited thickness[15]. Thus, they can bring in some attractive applications including wave focusing[16-18], selective mode transmission[19], mode conversion[20], cloaking[21] and so on. Among them, mode conversion and selective mode transmission are considered as the way to achieve one-way propagation control. In recent years, many researches

have been conducted to utilize metamaterials to realize the one-way transmission manipulation of waves[22-24]. Liang et al. used the ingenious combination of photonic crystal and nonlinear acoustic medium to innovatively propose a pioneer acoustic diode[25]. The theoretical model of the acoustic diode realized the unidirectional transmission of the acoustic energy flow. Zhu et al. proposed a slab structure via a symmetric-antisymmetric layout, and realized the one-way transmission of Lamb waves through the asymmetric mode conversion effect and Bragg scattering[26]. Through the mode conversion and the conversion efficiency of different diffraction orders, Li et al. achieved the systematically control the sound transmission of a sonic crystal by simply operating the mechanically rotating square rod[27]. Yang et al. proposed the use of fluid-like metamaterials and mode converters for efficient transmission of longitudinal waves to achieve unidirectional transmission of pure modes in the ultra-low frequency range[28]. Ding et al. put foward a composite Photonic Crystal (PC) plate composed of antisymmetric and symmetric PCs with periodic triangular bumps, and conducted experiments to verify the broadband unidirectional transmission phenomenon[29]. The state-of-the-art researches are generally limited to using the bandgap generated by Bragg scattering to achieve one-way propagation for a specific mode. However, metamaterials based on Bragg scattering usually face difficulty, considering their requirements in matching size with wavelength. Unlike Bragg scattering, elastic metamaterials based on the Local Resonance (LR) mechanism can easily realize the design of engineering structures with their sub-wavelength control capabilities. Therefore, it is necessary to explore new LR metamaterials for realizing the nonreciprocal transmission of Lamb waves.

In this paper, an elastic wave diode is proposed, composed of LR cylinders arranged in a periodic pattern bonded on an aluminum plate, which can realize broadband unidirectional manipulation of Lamb waves. The one-way transmission of single S_0 mode is explored. The mode conversion from S_0 mode to A_0 mode is realized by the antisymmetric unit cell. Selective mode transmission is realized by a symmetric unit cell layout. Furthermore, the effect of unit cell numbers of antisymmetric functional units on the mode conversion efficiency is studied. Subsequently, the effect of various shapes and structure sizes on the mode conversion efficiency is investigated. Finally, the optimal configuration of elastic wave diode is explored with harmonic analyses. The present paper is organized as follows: In Sec. 2, the band structure of symmetric unit metamaterial is investigated by modal analysis. Through investigating different vibration modes, a complete S waves bandgap is formed. The results of this part determine the operating frequency of the unidirectional propagation of this study. In Sec. 3, the optimal configuration of antisymmetric units is explored via the harmonic analysis of a finite element model (FEM), so that highly effective mode conversion from S_0 mode into A_0 mode can be achieved. In Sec.4, the frequency spectrum of the proposed elastic wave diode is obtained through FEM harmonic analysis to explore the energy transmission efficiency. In Sec. 5, the paper finishes with concluding remarks and suggestions for future work.

2. SYMMETRIC FUNCTIONAL UNITS FOR SINGLE MODE TRANSMISSION

This section presents the procedure and analysis for the symmetric metamaterial unit cell design. It demonstrates the mechanism of opening up complete symmetric mode bandgap.

2.1 Band structure of a symmetric functional unit

FIGURE 1(a) illuminates the schematic diagram of symmetric functional unit. It is constructed by a 2-mm thick aluminum plate and a double-sided aluminum-lead composite cylinder bounded on the plate. The radius r of the stubs is 1.75-mm and the lattice constant a of the unit cell is set to be 5 mm. The heights of aluminum and lead cylinders are separately 3 mm and 2.5 mm. In addition, the double-sided composite cylinder bonded on the aluminum plate can ensure the strong coupling of Lamb modes and stub modes based on local resonance mechanism, which can lead to the metamaterial structure capable of forming a wide resonant frequency spectrum[19]. The elastic properties of the materials used for the functional unit cells are as follows: elastic modulus $E_{Al} = 70$ Gpa; $E_{Pb} = 210$ Gpa; Poisson's ratio $\nu_{AL} = 0.33$; $\nu_{Pb} = 0.42$; density $\rho_{Al} = 2700\ kg/m^3$; $\rho_{Pb} = 11340\ kg/m^3$.

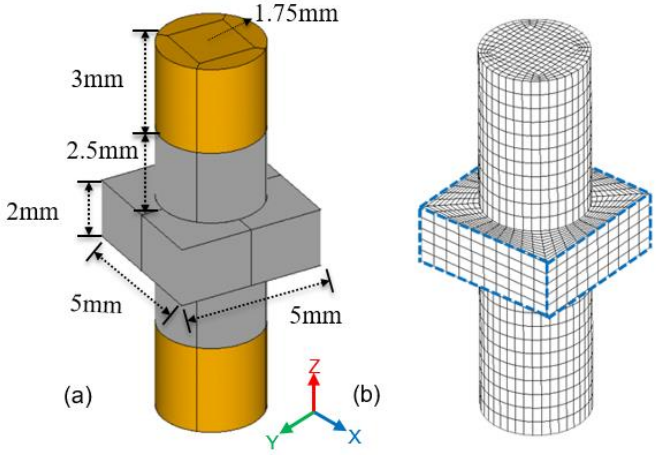

FIGURE 1 : (A) SYMMETRIC METAMATERIAL UNIT CELL SCHEMATIC DIAGRAM; (B) SYMMETRIC METAMATERIAL UNIT CELL FINITE ELEMENT MODEL

Bloch-Floquet periodic boundary condition is employed on the lateral surfaces of the unit cell using the finite element modeling (FEM) software package ANSYS 16.0 as presented in FIGURE 1(b). By periodic, it means that the material can be divided into finite-sized, identical, so-called periodic cells. Thus, one unit cell with Bloch-Floquet boundary condition can represent the entire structure.

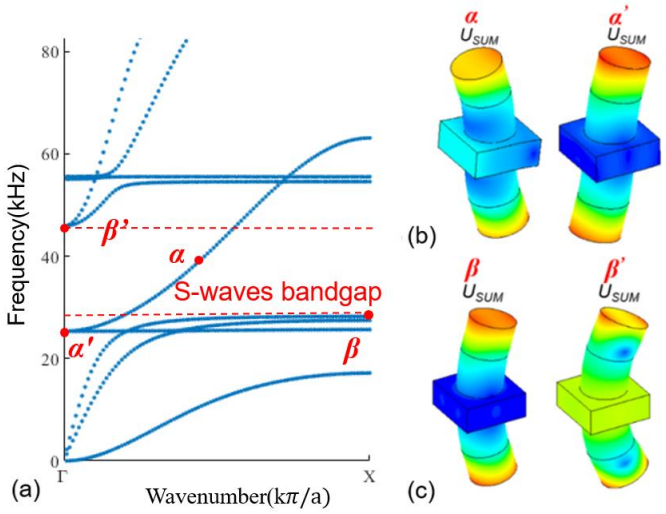

FIGURE 2: VIBRATION MODES OF BANDGAP EXTREMA:(A) THE DISPERSION RELATION OF THE UNIT CELL ALONG X DIRECTION FROM 0 TO 60 kHz; (B) THE PATTERNS PRESENTING THE DISPLACEMENT FIELD OF THE UNIT CELL RESONATING AT α AND α' MODES; (C) THE PATTERNS PRESENTING THE DISPLACEMENT FIELD OF THE UNIT CELL RESONATING AT β AND β' MODES

2.2 Mechanism for S waves bandgap formation

The selective guided wave mode transmission is achieved by the bandgap behavior of different stub modes as well as the coupling between these stub modes with the desired Lamb modes.

FIGURE 2(a) shows that the dispersion curves of the metamaterial are considerably complex due to the strong coupling and interactions between wave motions in the plate and the stub structures. FIGURE 2(b) displays the stub modes and Lamb modes of the unit cells at 40 kHz (the location of the red circle) within band range. It can be noticed that both structures vibrate following an antisymmetric motion with respect to the plate mid-plane, representing a strong coupling between this stub mode and the antisymmetric Lamb mode. On the other hand, the symmetric Lamb motion is totally decoupled with such a kind of stub motion. In other words, only antisymmetric modes are allowed transmitting through the metamaterial interface, forming a symmetric mode bandgap. FIGURE 2 (c) presents the extrema of the wave motions bounding the S-mode bandgap, with the degenerate anti-resonance α followed by the corresponding resonance α'. The anti-resonances are defined by the fact that the vibrational amplitude at the bottom of the stub becomes zero, indicating the transmission along the plate becomes prohibited. Otherwise, the resonances correspond to the cutting-in of a wave mode, representing the starting point of effective wave transmission. S-mode bandgap is formed by the strong anti-resonant coupling between the S_0 plate motion and the symmetric stub motion as β. In this manner, the propagation of the symmetric modes will be prevented, forming a complete S-mode bandgap from 27.48 kHz up to the cut-in frequency at 44.15 kHz defined by the resonant mode β'.

The complete S-mode bandgap leads to the possibility of selectively transmitting antisymmetric Lamb mode into the host plate structure. It is the first step towards nonreciprocal transmission.

3. ANTISYMMETRIC FUNCTIONAL UNITS DESIGN

This section presents the procedure and analysis for the antisymmetric metamaterial unit cell design. A series of parametric study is conducted to determine the optimal configuration. The parametric studies are divided into three parts including the periodic cell numbers of antisymmetric unit cells, the height of cylinder stub, and the shape of surface-bonded cell.

3.1 Unit cell configuration

FIGURE 3(a) illuminates the schematic diagram of the proposed metamaterial unit cell. It is comprised of double-sided lead cylinders bonded on a 2-mm thickness host aluminum plate in a fashion of an antisymmetric layout. Aluminum and lead are chosen for the design, since both materials are easily accessible and can be readily machined. The radius r of the stubs is 1.75-mm and the lattice constant a of the unit cell is set to be 5 mm. The optimal height of cylinder will be determined from next part. As antisymmetric structures, these units will generate antisymmetric displacement response when excited by symmetrical load. Thus, it provides the possibility of mode conversion from symmetric Lamb modes into antisymmetric Lamb modes. FIGURE 3(b) presents the 3D and top views of the finite element model used for computing the frequency spectra.

3.2 Optimal configuration design

To explore the optimal configuration of mode converter constructed by the periodic antisymmetric units, it is necessary to ensure the evolution relationship between numbers of unit cells and the mode conversion efficiency.

Harmonic analysis was conducted to obtain the spectral response of the n × 1 unit-cell-chain model and evaluate the mode conversion performance of the metamaterial structure. In this parametric study, n will range from 1 to 10. FIGURE 4 presents the numerical model setups, representing a pristine homogeneous plate and a sample metasystem with nine antisymmetric functional units. Line source of 10-N external force orientating along X direction was applied on both the top and bottom surfaces, 100 mm from the left boundary of the metamaterial functional unit to generate an incident Lamb waves with the fundamental symmetric mode into the structure. To absorb the boundary reflections and minimize the computational burden, two non-reflective boundaries (NRBs) were implemented on both ends of the structures[30]. The transmittance was evaluated by taking the averaged in-plane displacements at the sensing points located along the detection line 100 mm away from the right side of the metasurface. The

transmission ratio ξ and mode conversion ratio η are defined as

$$\xi = S_m / S_p \quad (1)$$

$$\eta = A_m / S_p \quad (2)$$

where S_m is the magnitude of symmetric Lamb waves after transmitting through the metamaterial structure; and S_p represents the magnitude for the pristine homogenous plate. And A_m is the magnitude of antisymmetric Lamb waves after the metamaterial manipulation.

The magnitude of symmetric Lamb wave is calculated by taking the average of in-plane displacements of top and bottom sensing points. And the magnitude of antisymmetric Lamb wave is calculated by taking average of the difference of in-plane displacement of both sensing points.

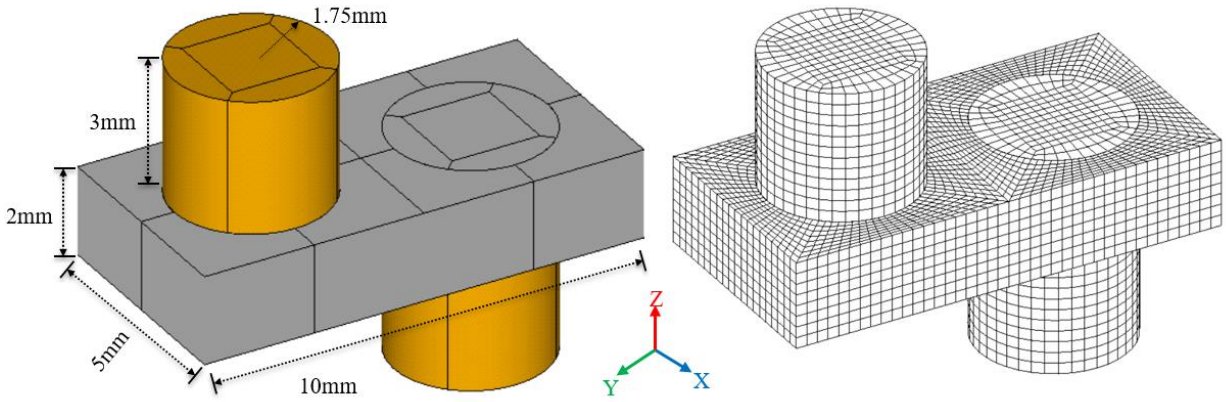

FIGURE 3: (A) ANTISYMMETRIC METAMATERIAL UNIT CELL SCHEMATIC DIAGRAM; (B) ANTISYMMETRIC METAMATERIAL UNIT CELL FINITE ELEMENT MODEL

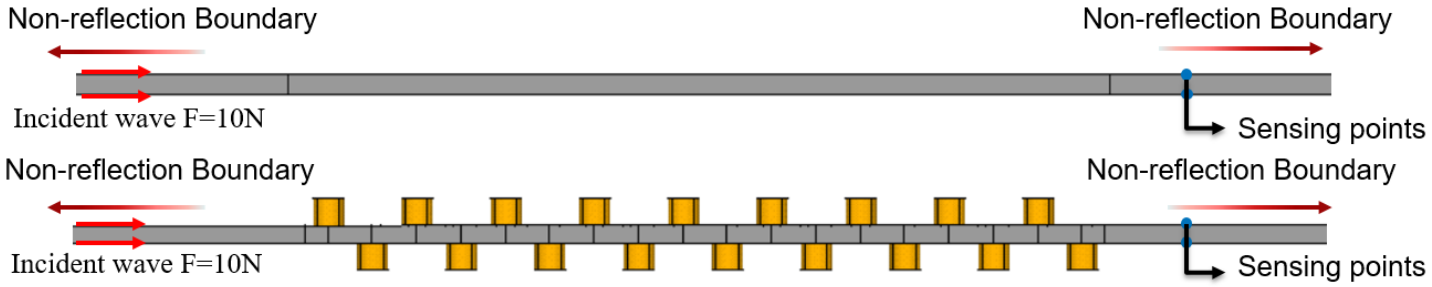

FIGURE 4: MODEL LAYOUT OF THE METASYSTEM: (A) A PRISTINE HOMOGEOUS PLATE; (B) METASURFACE WITH NINE FUNCTIONAL UNITS

FIGURE 5 shows the mode conversion ratio curves from the parametric case studies. It can be seen that in the frequency range from 20 kHz to 80 kHz, the structure composed of only one antisymmetric unit achieved good performance in a wide frequency range. The cases of this parametric study took the units of the same geometric constant. As the number of periodic units increases, the evolution trend of mode conversion ratio gradually converges. This means that as the periodic number increases, although the conversion rate from symmetric Lamb mode into antisymmetric Lamb mode may have increased, yet the final converted mode energy transmission stayed low due to multiple reflections at each unit cell. Therefore, when only one antisymmetric unit structure is applied as the mode convertor, the balance between transmittance and conversion efficiency can be achieved. And under the operating frequency range obtained in section 2, an anti-symmetric unit can achieve mode conversion efficiency up to 23%, far exceeding other cases. To sum up, only one antisymmetric unit will be chosen as the mode converter to achieve the optimal mode conversion.

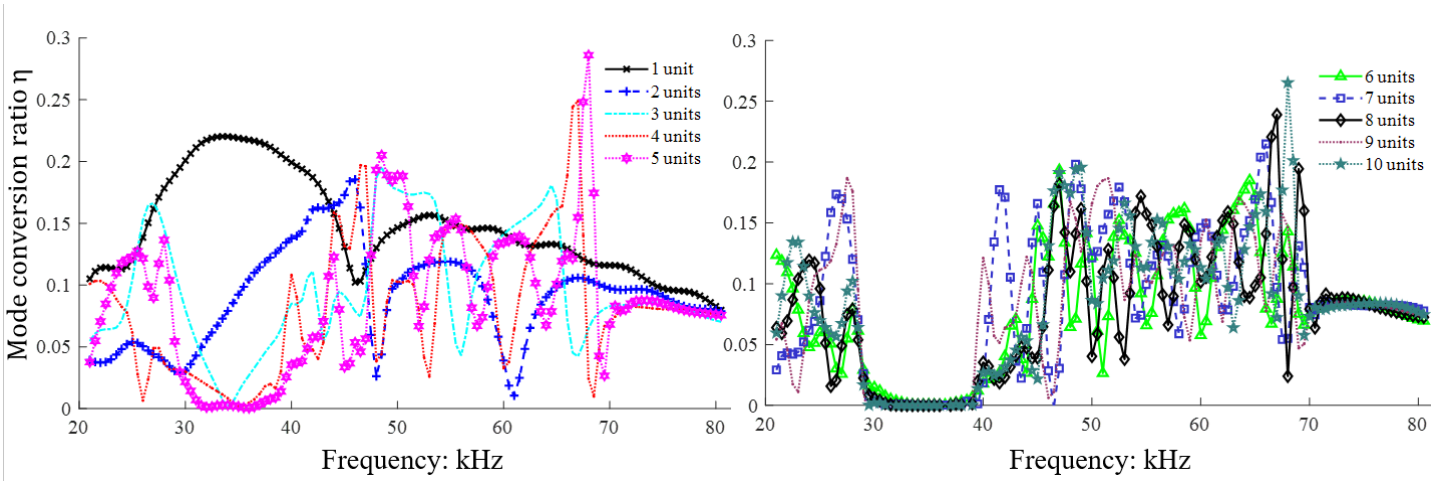

FIGURE 5: MODE CONVERSION RATIO CURVES OF METASYSTEMS WITH DIFFERENT NUMBER OF FUNCTIONAL UNITS (A) CASES FROM 1 UNIT TO 5 UNITS; (B) CASES FROM 6 UNITS TO 10 UNITS

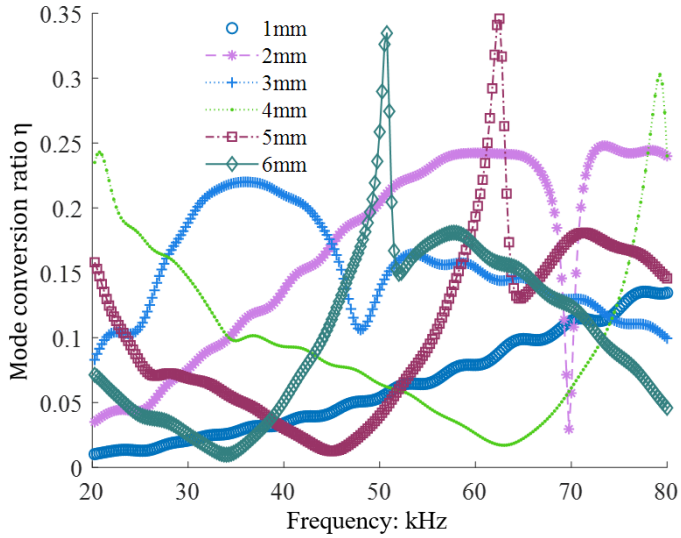

FIGURE 6: MODE CONVERSION RATIO CURVES OF THE METASYSTEMS BY ADJUSTING THE CYLINDER STUB HEIGHT FROM 1MM TO 6 MM WITH A STEP OF 1 MM

Subsequently, the relationship between the height of cylinder stub and mode conversion efficiency needs to be explored. Harmonic analysis was conducted to obtain the spectral response of metasystem. According to the previous conclusion, the metasystem is constructed by only one functional unit. In this part of parametric study, six cases of the cylinder height from 1mm to 6 mm were evaluated with a step of 1mm. FIGURE 6 presents the mode conversion ratio of six parametric study cases from 1mm to 6mm. It shows that the antisymmetric unit with 3mm cylinder stub possesses the optimal performance in the frequency range from 20 kHz to 45 kHz. It should be noted that as the height of the cylinder increases, the development trend of the conversion efficiency also follows a certain pattern. It seems to shift the conversion function peaks towards the lower frequency range. Based on the previous conclusion, the optimal figuration of mode conversion efficiency can be achieved in the specified frequency range.

4. ELASTIC WAVE DIODE PERFORMANCE

Enlightened by the classical one-way wave propagation control method, a two-component design was arrived, namely the mode convertor with the mode selector, forming the elastic wave diode. According to the previous results, the symmetric structure unit was employed as the mode selector to realize the selective transmission of the anti-symmetric Lamb modes, and prohibit the propagation of the symmetric modes in the specific frequency range. The aforementioned one anti-symmetric unit was utilized to realize the conversion from symmetric modes to anti-symmetric modes. By combining such two unit structural components, the non-reciprocal propagation of symmetric Lamb waves can be realized.

FIGURE 7 presents the schematic diagram for both forward and backward wave transmission cases. When the elastic wave diode is in the forward excitation state, the symmetrical mode Lamb waves passes through the mode converter firstly, so that part of the symmetrical mode is converted into antisymmetric modes. While the residual symmetric mode Lamb waves passing through the mode selector, the motion will be prohibited by its bandgap behavior. On the other hand, the converted antisymmetric Lamb wave will pass through the selector. Conversely, when the elastic wave diode is functioning in the backwards case, all symmetric mode Lamb waves will be stopped directly by the mode selector with zero energy allowed for transmission. Therefore, nonreciprocal propagation control for symmetric Lamb waves is achieved. Harmonic analyses were conducted to demonstrate the one-way propagation performance of elastic wave diode. Symmetric and antisymmetric modes are quantified in the same way as the previous sections.

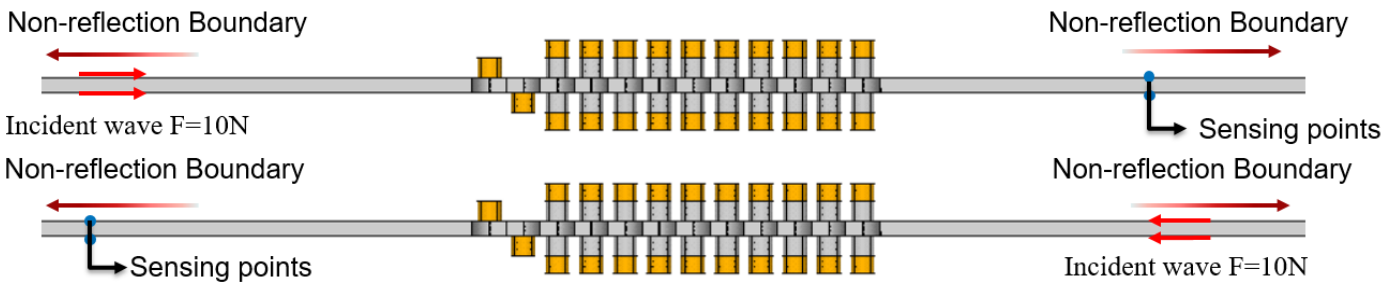

FIGURE 7: SCHEMATIC DIAGRAMS FOR FORWARD AND BACKWARD PROPAGATION CASES

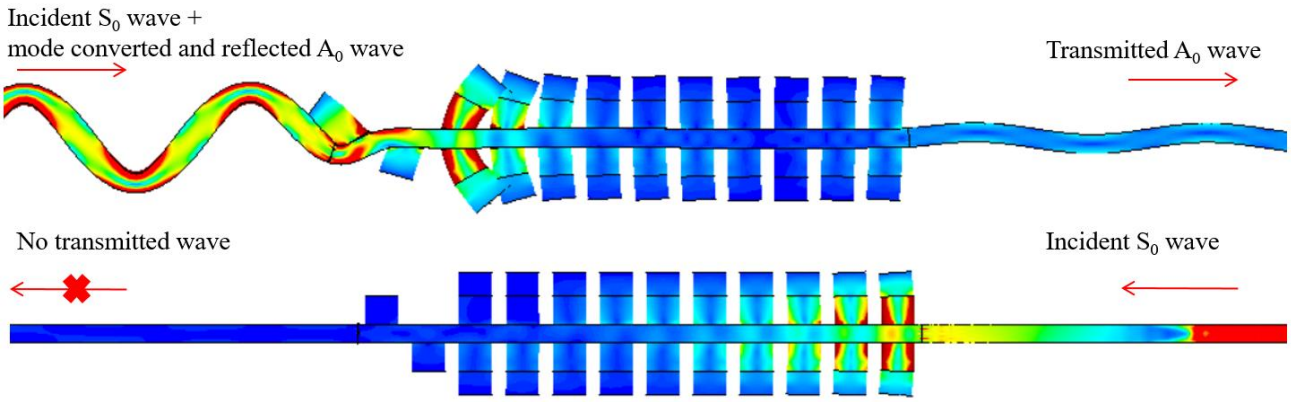

FIGURE 8: DISPLACEMENT FIELDS OF ELASTIC WAVE DIODE UNDER FORWARD DIRECTION EXITATION AND BACKWARD DIRECTION EXCITATION

FIGURE 8 shows the displacement fields of unit-chain models for forward and backward wave propagation cases respectively. Transmitted antisymmetric Lamb modes can be clearly observed in the forward propagation scenario. And the nonreciprocal transmission effect is evidently shown by the comparison of displacement fields, since no backward transmission was captured. It was worth mentioning that during forward transmission, the antisymmetric vibration mode was also presented at the left-hand side of the metasurface due to mode conversion and the reflection from the convertor cell.

FIGURE 9 shows the transmitted amplitudes of antisymmetric and symmetric Lamb waves. Green and red lines present the transmission spectra of forward propagation case, blue and brown lines denote those of the backward propagation case. The difference in amplitude between the red line and the blue line in FIGURE 9 indicates a comparison between the reception of forward and backward propagation. When entering the bandgap frequency of backward propagation, there is no displacement response at the diode receiving end. At the same time, it can be clearly seen that in this frequency band, the receiving end of the forward propagation case exhibits a relatively high amplitude of antisymmetric modes. FIGURE 9 demonstrates that, within the specified frequency range from 28 kHz to 42 kHz, a significant difference can be found in the displacement responses for forward and backward wave propagation scenarios, the extrema magnitude ratio reaches 25 times.

In order to further improve the conversion efficiency of elastic wave diode, the number of periodic unit cells was further adjusted in the symmetrical structure to 6, 8, 10, and 12 respectively. FIGURE 10 shows the Lamb wave amplitudes of these four cases. FIGURE 10 (a) to (d) respectively show the cases of 6, 8, 10, 12 symmetrical units. It is apparent that with the increase of the number of symmetric unit cells, the bandgap effect enjoyed enhancements on the symmetric mode Lamb wave filtration. When the number of symmetric elements is sufficient, a complete bandgap will be formed. However, the increase in the number of periods will inevitably lead to the weakening of wave transmittance, which eventually leads to reduction in the one-way propagation efficiency. Therefore, the balance between the bandgap effect and the energy transmittance effect should be achieved.

To quantitatively evaluate the efficiency of unidirectional propagation, the energy flux measurements were conducted, which computes the sum of kinetic and potential energies on the receiving cross section. Lamb wave kinetic energy and potential energy was defined as[31]

$$k_e = \frac{1}{2}\rho\int_A (v_x^2 + v_y^2)dA \tag{3}$$

$$v_e = \frac{1}{2}\int_A (T_{xx}S_{xx} + T_{YY}S_{YY} + 2T_{XY}S_{XY})dA \tag{4}$$

where v presents the velocity, T denotes the mechanical stress, and S strands for the elastic strain.

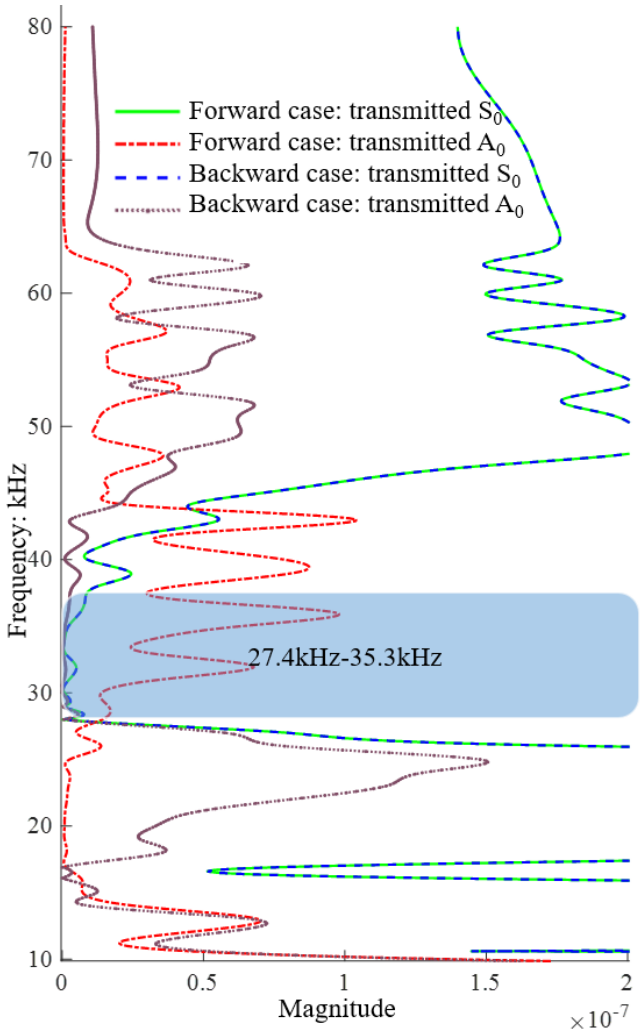

FIGURE 9: LAMB WAVES TRANSMISSION SPECTRA FOR S_0 WAVE FORWARD AND BACKWARD PROAPGATION CASES

According to wave mechanics theory, the kinetic energy and potential energy at the same cross section are equal. The same method is used to calculate the energy flow of symmetric mode and antisymmetric mode respectively. Therefore, the ratio of the propagating energy of waves of different modes can be quantitatively compared in this manner. In particular, the ratio between the forward transmission energy to the backward transmission energy was evaluated. Such a ratio implies the one-way propagation effectiveness of the diode. The larger the ratio of energy transmission, the better the diode is for the one-way wave control. The ratios of unidirectional wave propagation efficiency for a diode composed of 1 antisymmetric unit with 8, 10, and 12 symmetric unit cells were explored. The developing trend of the results shown in FIGURE 11 is similar to FIGURE 10, and the peak value can reach as high as 6000 for the 10 symmetric unit cell case, which means the successful non-reciprocal propagation through the proposed elastic wave diode.

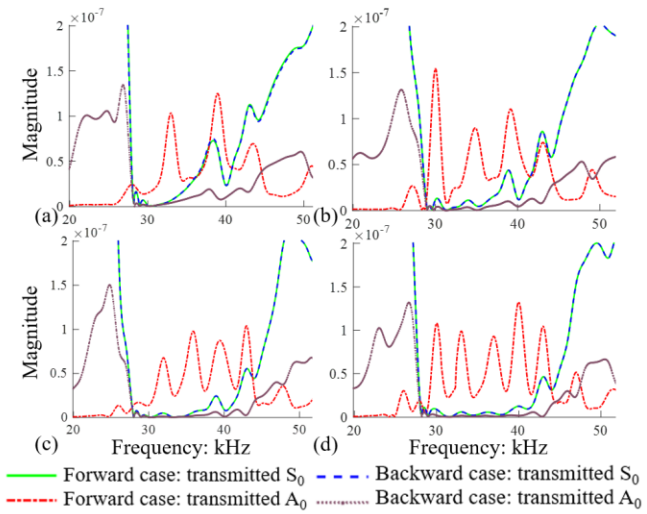

FIGURE 10: LAMB WAVE TRANSMISSION SPECTRA OF THE ELASTIC WAVE DIODE (BLUE LINE: FORWARD PROPAGATION CASE S_0 TRANSMISSION AMPLITUDE; RED LINE: FORWARD PROPAGATION CASE A_0 TRANSMISSION AMPLITUDE; GREEN LINE: BACKWARD PROPAGATION S_0 TRANSMISSION AMPLITUDE; BROWN LINE: BACKWARD PROPAGATION A_0 TRANSMSSION AMPLITUDE)

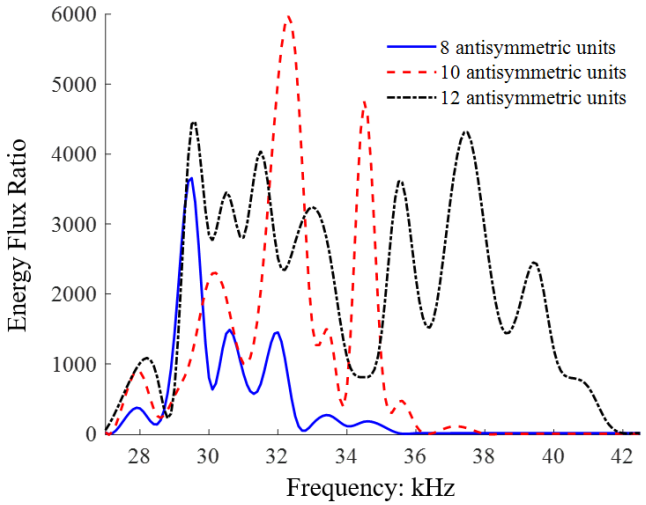

FIGURE 11: ENERGY FLUX RATIO OF ELASTC WAVE DIODE

5. CONCLUDING REMARKS AND FUTURE WORK

In conclusion, an effective approach to obtain elastic wave diode was proposed, which achieved symmetric Lamb wave reciprocal transmission. The mechanism behind the metamaterial elastic wave diode resides in the wave mode manipulation, including mode conversion and selective mode transmission. The final metamaterial guided wave diode combines one antisymmetric functional unit and ten symmetric functional units. Parametric studies determined the optimal design figurations. Furthermore, the balance between

transmission and bandgap effect was realized. Numerical case studies demonstrated the effectiveness of the one-way manipulation capability of the elastic diode via the energy flux computation. For future work, the elastic wave diode should be integrated with SHM/NDE applications or novel transducer designs.

6. ACKNOWLEDGEMENTS

The support from the National Natural Science Foundation of China (contract numbers 51975357 and 51605284) is thankfully acknowledged; this research is also sponsored by the Shanghai Rising-star Program (contract number 21QA1405100).

REFERENCES

[1] Kundu, T., Schmidt, D., Sadri, H., Szewieczek, A., Sinapius, M., Wierach, P., Siegert, I., and Wendemuth, A., 2013, "Characterization of Lamb wave attenuation mechanisms," Health Monitoring of Structural and Biological Systems 2013,pp,9-16.

[2] Wan, X., Xu, G., Zhang, Q., Tse, P. W., and Tan, H., 2016, "A quantitative method for evaluating numerical simulation accuracy of time-transient Lamb wave propagation with its applications to selecting appropriate element size and time step," Ultrasonics, 64, pp. 25-42.

[3] Zheng, Y., Liu, K., Wu, Z., Gao, D., Gorgin, R., Ma, S., and Lei, Z., 2019, "Lamb waves and electro-mechanical impedance based damage detection using a mobile PZT transducer set," Ultrasonics, 92, pp. 13-20.

[4] Wu, X.-H., Shen, Y.-P., and Sun, Q., 2007, "Lamb wave propagation in magnetoelectroelastic plates," Applied Acoustics, 68(10), pp. 1224-1240.

[5] Kundu, T., Luangvilai, K., Jacobs, L. J., and Qu, J., 2005, "Modal decomposition of double-mode Lamb waves: numerical verification and discussion on extension to general multimode leaky Lamb waves," Health Monitoring and Smart Nondestructive Evaluation of Structural and Biological Systems IV, pp. 304-312.

[6] Chen, X., and Wang, C., 2015, "Tsallis Distribution-Based Fractional Derivative Method for Lamb Wave Signal Recovery," Research in Nondestructive Evaluation, 26(3), pp. 174-188.

[7] Li, B., Alamri, S., and Tan, K. T., 2017, "A diatomic elastic metamaterial for tunable asymmetric wave transmission in multiple frequency bands," Sci Rep, 7(1), p. 6226.

[8] Zeng, L.-S., Shen, Y.-X., Peng, Y.-G., Zhao, D.-G., and Zhu, X.-F., 2021, "Selective Topological Pumping for Robust, Efficient, and Asymmetric Sound Energy Transfer in a Dynamically Coupled Cavity Chain," Physical Review Applied, 15(6).

[9] Guo, X.-F., and Ma, L., 2020, "One-way transmission in topological mechanical metamaterials based on self-locking," International Journal of Mechanical Sciences, 175.

[10] Chen, Y., and Wang, L., 2015, "Multiband wave filtering and waveguiding in bio-inspired hierarchical composites," Extreme Mechanics Letters, 5, pp. 18-24.

[11] Li, B., and Tan, K. T., 2016, "Asymmetric wave transmission in a diatomic acoustic/elastic metamaterial," Journal of Applied Physics, 120(7).

[12] Shu, H., Xu, L., Shi, X., Zhao, L., and Zhu, J., 2016, "Traveling Lamb wave in elastic metamaterial layer," Journal of Applied Physics, 120(16).

[13] Goh, H., and Kallivokas, L. F., 2020, "Inverse band gap design of elastic metamaterials for P and SV wave control," Computer Methods in Applied Mechanics and Engineering, 370.

[14] Zhu, R., Liu, X. N., Hu, G. K., Sun, C. T., and Huang, G. L., 2014, "Negative refraction of elastic waves at the deep-subwavelength scale in a single-phase metamaterial," Nat Commun, 5, p. 5510.

[15] Park, J. H., Lee, H. J., and Kim, Y. Y., 2016, "Characterization of anisotropic acoustic metamaterial slabs," Journal of Applied Physics, 119(3).

[16] Zhu, H., and Semperlotti, F., 2016, "Anomalous Refraction of Acoustic Guided Waves in Solids with Geometrically Tapered Metasurfaces," Phys Rev Lett, 117(3), p. 034302.

[17] Jin, Y., Wang, W., Khelif, A., and Djafari-Rouhani, B., 2021, "Elastic Metasurfaces for Deep and Robust Subwavelength Focusing and Imaging," Physical Review Applied, 15(2).

[18] Zhu, Y., Cao, L., Merkel, A., Fan, S.-W., and Assouar, B., 2020, "Bifunctional superlens for simultaneous flexural and acoustic wave superfocusing," Applied Physics Letters, 116(25).

[19] Tian, Y., and Shen, Y., 2020, "Selective guided wave mode transmission enabled by elastic metamaterials," Journal of Sound and Vibration, 485.

[20] Yang, X., Chai, Y., and Li, Y., 2021, "Metamaterial with anisotropic mass density for full mode-converting transmission of elastic waves in the ultralow frequency range," AIP Advances, 11(12).

[21] Ning, L., Wang, Y.-Z., and Wang, Y.-S., 2020, "Active control cloak of the elastic wave metamaterial," International Journal of Solids and Structures, 202, pp. 126-135.

[22] Ansari, M. H., Attarzadeh, M. A., Nouh, M., and Karami, M. A., 2018, "Application of magnetoelastic materials in spatiotemporally modulated phononic crystals for nonreciprocal wave propagation," Smart Materials and Structures, 27(1).

[23] Fleury, R., Sounas, D. L., Sieck, C. F., Haberman, M. R., and Alu, A., 2014, "Sound isolation and giant linear nonreciprocity in a compact acoustic circulator," Science, 343(6170), pp. 516-519.

[24] Trainiti, G., and Ruzzene, M., 2016, "Non-reciprocal elastic wave propagation in spatiotemporal periodic structures," New Journal of Physics, 18(8).

[25] Liang, B., Guo, X. S., Tu, J., Zhang, D., and Cheng, J. C., 2010, "An acoustic rectifier," Nat Mater, 9(12), pp. 989-992.

[26] Zhu X, Zou X, Liang B, and Cheng, J. C., 2010, "One-way mode transmission in one-dimensional phononic crystal plates," Journal of Applied Physics, 108(12).

[27] Li, X. F., Ni, X., Feng, L., Lu, M. H., He, C., and Chen, Y. F., 2011, "Tunable unidirectional sound propagation through a sonic-crystal-based acoustic diode," Phys Rev Lett, 106(8), p. 084301.

[28] Yang, X., Yao, S., Chai, Y., and Li, Y., 2021, "Efficient pure-mode elastic mode-converting diode," Journal of Physics D: Applied Physics, 54(36).
[29] Ding, T., Song, A., Sun, C., Xiang, Y., and Xuan, F.-Z., 2022, "Mode conversion of Lamb waves in a composite phononic crystal plate: Numerical analysis and experimental validation," Journal of Applied Physics, 132(22).
[30] Shen, Y., and Giurgiutiu, V., 2015, "Effective non-reflective boundary for Lamb waves: Theory, finite element implementation, and applications," Wave Motion, 58, pp. 22-41.
[31] Kamal, A. M., Lin, B., and Giurgiutiu, V., 2013, "Exact analytical modeling of power and energy for multimode lamb waves excited by piezoelectric wafer active sensors," Journal of Intelligent Material Systems and Structures, 25(4), pp. 452-471.